Medicinal Chemistry, 2018, *14*, 809-817

RESEARCH ARTICLE

Identification of New Chromenone Derivatives as Cholinesterase Inhibitors and Molecular Docking Studies

Jamshed Iqbal[a,*], Muhammad S.A. Abbasi[b], Sumera Zaib[a], Saifullah Afridi[a], Norbert Furtmann[c], Jürgen Bajorath[c] and Peter Langer[b]

[a]*Centre for Advanced Drug Research, COMSATS Institute of Information Technology, Abbottabad, Abbottabad-22060, Pakistan;* [b]*Institut für Chemie, Universität Rostock, Albert Einstein Str. 3A, 18059 Rostock, Germany;* [c]*Department of Life Science Informatics, B-IT, LIMES Program Unit Chemical Biology and Medicinal Chemistry, Rheinische Friedrich-Wilhelms-Universität, Dahlmannstr. 2, D-53113 Bonn, Germany*

ARTICLE HISTORY

Received: September 16, 2017
Revised: January 27, 2018
Accepted: January 29, 2018

DOI:
10.2174/1573406414666180222091833

Abstract: ***Background*:** Alzheimer's Disease (AD) is the leading cause of dementia among the aging population. This devastating disorder is generally associated with the gradual memory loss, specified by a decrease of acetylcholine level in the cortex hippocampus of the brain due to hyperactivation of cholinesterases (acetylcholinesterase (AChE) and butyrylcholinesterase (BChE)).

***Objective*:** Therefore, inactivation of AChE and BChE by inhibitors can increase the acetylcholine level and hence may be an encouraging strategy for the treatment of AD and related neurological problems.

***Method*:** In this contribution, two series of chromenone-based derivatives were tested by Ellmann's calorimetric method for AChE and BChE inhibition.

***Results*:** All the compounds showed inhibitory activity against cholinesterases and some of them exhibited dual inhibition of AChE as well as BChE. The most potent inhibitor of AChE was **2l** having an IC_{50} value of 0.08 ± 0.03 µM, while **3q** inhibited the BChE with an IC_{50} value of 0.04 ± 0.01 µM. In case of dual inhibition, **3h** showed an inhibitory concentration of 0.15 ± 0.01 µM for AChE, and 0.09 ± 0.01 µM for BChE. Molecular docking studies were performed to explore the probable binding modes of the most potent dual inhibitors.

***Conclusion*:** It can be hypothesized that the inhibitors are able to target cholinesterase pathways and may emerge as a suitable outset for the further development process.

Keywords: Alzheimer's disease, amino acid, chromosome, chromenone derivatives, cholinesterase inhibitor, molecular docking.

1. INTRODUCTION

Cholinesterases (ChEs) are a family of esterase/lipase enzymes that share extensive sequence homology and catalyze the hydrolysis of acetylcholine (ACh). To terminate the desired cholinergic-transmission, ChEs catalyze the acetylcholine breakdown into choline and acetic acid [1-3]. Based on specificities of substrates and inhibitors, different vertebrate ChEs include acetylcholinesterase (AChE) and butyrylcholinesterase (BChE). Amino acid sequence homology in AChE and BChE is 65% although they are encoded by different genes on the human chromosome (AChE: 7q22, BChE: 3q26) [4]. AChE (EC 3.1.1.7) is a key enzyme involved in neurotransmission located at all autonomic ganglia, cholinergic brain synapses and neuromuscular junctions, and plays a crucial role in the termination of signal transmission by hydrolyzing ACh [3, 5, 6]. AChE also acts as an adhesion protein in bone matrix, as well as supporting neurite growth and amyloid fibrils production, mostly found in the brain cells of Alzheimer's patients [3, 7, 8]. Currently, the inhibition of ChEs represents a promising strategy for the symptomatic treatment and management of AD [9]. Cholinergic neurons are mainly located in regions of the forebrain that are associated with learning and memory [10] and hippocampus [11]. By inhibiting AChE the degradation of ACh is reduced, and in this way, ACh levels can be elevated, which results in improved learning and memory functions. The irreversible deficiency of cholinergic transmitters is the main cause of memory impairment in patients suffering from senile dementia, therefore, AChE inhibitors can be employed at the early stage of AD treatment [12].

*Address correspondence to this author at the Centre for Advanced Drug Research, COMSATS Institute of Information Technology, Abbottabad, Postal Code-22060, Pakistan; Tel: +92-992-383591-96; Fax: +92-992-383441; E-mails: drjamshed@ciit.net.pk; jamshediqb@googlemail.com

1875-6638/18 $58.00+.00

Pseudocholinesterase or BChE (E.C. 3.1.1.8), also known as plasma cholinesterase, is mostly found in the liver and participates in the control of neurotransmission [7]. It is reported that BChE contributes about 20% and AChE accounts for 80% of total cholinesterase activity in healthy brains. In patients suffering from AD, the activity of BChE is found to increase to about 40% [4, 7].

A characteristic feature of AD patients is the presence of neurofibrillary tangles (NFT) and β-amyloid plaques, in which large quantities of ChEs are found, more specifically BChE. Therefore, the possible involvement of ChEs in the formation of tangles and plaques activates the microglia and thus hydrolyzes acetylcholine [13]. Hence, ChE inhibitors not only play a role to enhance the function of the damaged brain, but also help in the prevention of further degeneration [12, 14]. AChE and BChE inhibitors are considered for the treatment of AD patients. While existing medications (donepezil, tacrine and rivastigmine) target AChE, there is currently no medication available targeting BChE [4]. Therefore, there is a growing interest in the development of cholinesterase inhibitors for the therapy of Alzheimer's and related neurological problems.

Very recently, hybrid compounds such as acridine-chromenones, quinoline-chromenones, and triazole-chromenones have been developed as new anti-Alzheimer's agents [15, 16]. However, most of these hybrid compounds exhibit only moderate potency against AChE. In view of these findings, and to expand the scope of the chromenone skeleton in medicinal chemistry as anti-Alzheimer's agents, we introduce herein structurally diverse chromenone derivatives with modular substitution pattern. These compounds were more easy to access compared to larger hybrid molecules reported in the literature [15, 16]. Cholinesterase inhibitory activity was evaluated and molecular docking studies were carried out to explore the probable binding modes of potent dual inhibitors identified in this study.

2. MATERIALS AND METHODS

2.1. Synthesis of 6-oxo-6*H*-benzo[*c*]chromene-8,10-dicarboxylate Derivatives

A general scheme and procedure for the synthesis of a novel series of 6-oxo-6*H*-benzo[*c*]chromene-8,10-dicarboxylate derivatives (**2a-n**) have been reported in a previous publication [17].

2.2. Synthesis of 6*H*-benzo[*c*]chromen-6-ones Derivatives

A general scheme and procedure for the synthesis of a novel series of 6*H*-benzo[*c*]chromen-6-ones (**3a-w**) have also been reported previously [18].

2.3. Materials and Chemicals

AChE (from electric eel) BChE (from horse serum), acetylthiocholine chloride and butyrylthiocholine chloride and DTNB were purchased from Sigma Aldrich (St. Louis, MO, USA) and other chemicals were of analytical grade.

2.4. Cholinesterase Inhibition Studies

The capacity to inhibit cholinesterase activity was determined by Ellmann's calorimetric method [19] with slight modifications [5]. The reaction mixture contained 60 µL phosphate buffer (KH_2PO_4/ KOH), pH 7.7, 10 µL of enzyme (0.015 units per well for AChE & BChE) and 10 µL of test compound (prepared in 1% DMSO and diluted in the buffer). All the contents were mixed thoroughly and incubated for 10 min at 37 °C. The enzymatic reaction was initiated by the addition of 10 µL of respective substrates (1 mM acetylthiocholine chloride or butyrylthiocholine chloride) to their enzyme solutions. After that 10 µL of coloring reagent 5,5'-dithiobis(2-nitrobenzoic acid) (DTNB; 0.5 mM) was added. The mixture was incubated at 37 °C for 20 min and the absorbance was measured at 405 nm using a 96-well microplate reader (BioTek ELx800, Instruments, Inc. USA). Blank controls without enzymes were also prepared in order to check the non-enzymatic hydrolysis of substrates. The experiments were carried out in triplicate. Galanthamine (0.1 mM) was used as a standard inhibitor. Similarly, to determine the enzyme activity, the reaction without inhibitor was performed. The percentage inhibition was calculated by the following formula:

$$\% \text{ age inhibition} = 100-(Ac/Af) \times 100$$

Where "Ac" and "Af" are the absorbance of inhibitor and control (without inhibitor) minus their respective pre-read absorbance. The compounds that revealed more than 50% inhibition for AChE/BChE were further diluted to eight different concentrations for the assessment of IC_{50} values (GraphPad PRISM 5.0, San Diego, California, USA).

2.5. Molecular Docking Studies

The X-ray structures of human AChE (PDB ID: 4BDT) [20] in complex with huprine W and BChE (PDB ID: 4BDS) [20] in complex with tacrine were obtained from the RCSB Protein Bank [21]. These structures were used as templates for flexible ligand docking with AutoDock 4.2 [22]. In the case of AChE, residue Tyr337 was flexible during docking while all other residues were held fixed in their crystallographic conformation. In the case of BChE, the entire active site was kept rigid including residue Ala328, which corresponds to Tyr337 in AChE. Prior to docking, crystallographic ligand and water molecules were removed from the X-ray structures and explicit hydrogen atoms were added using the Molecular Operating Environment (MOE 2012.10) [23]. Atomic partial charges were calculated using AutoDock Tools [22]. Selected chromone derivatives were docked into the active sites of AChE and BChE using AutoDock 4.2 with standard parameter settings. Based on visual inspection, high-scoring docking poses were selected as putative binding modes.

3. RESULTS AND DISCUSSION

3.1. Synthesis of 6-oxo-6*H*-benzo[*c*]chromene-8,10-dicarboxylate Derivatives

The synthetic route adopted for the preparation of 6-oxo-6*H*-benzo[*c*]chromene-8,10-dicarboxylate derivatives (**2a-n**) is illustrated in Scheme **1**. The physicochemical properties

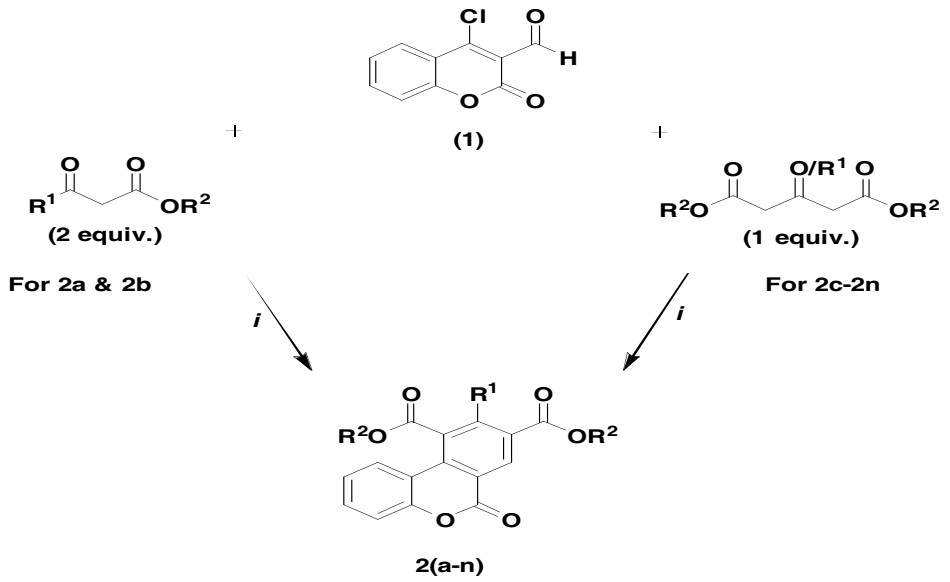

Scheme 1. Synthesis of 6*H*-benzo[*c*]chromen-6-ones **2(a-n)**; Reagents and conditions: (*i*) K_2CO_3, THF, 50 °C, 2h (**2a &2b**) and 4-8 h (**2c-2n**).

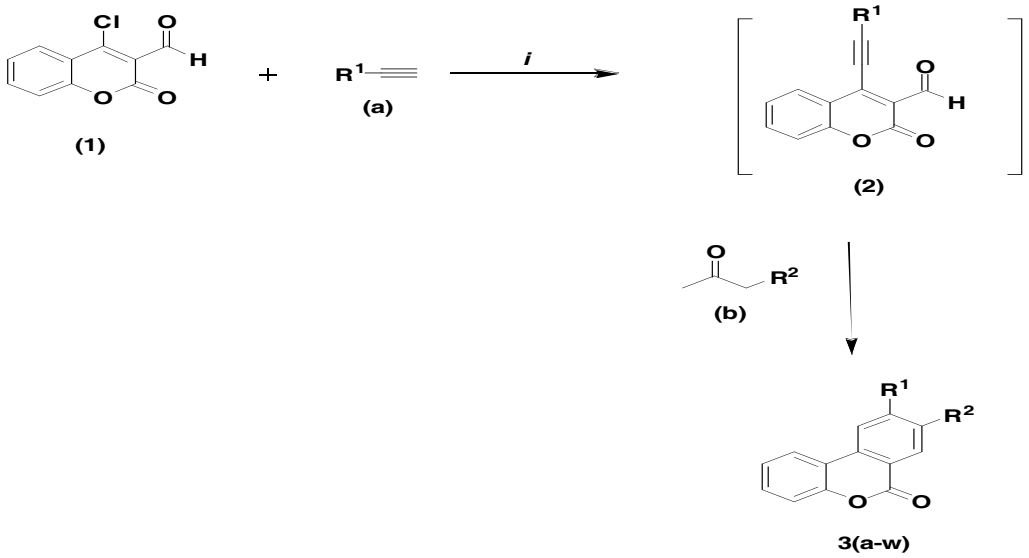

Scheme 2. Synthesis of compounds **3(a-w)**; Reagents and Conditions; (*i*) $PdCl_2(PPh_3)_2$, CuI, THF, K_2CO_3, 20-50 °C, 5-10 h.

and their spectroscopic data were reported in our previous publication [17]. All variations of substituents R^1 & R^2 are shown in Table **1**.

3.2. Synthesis of 6*H*-benzo[*c*]chromen-6-ones Derivatives

The synthetic route adopted for the preparation of 6*H*-benzo[*c*]chromen-6-ones derivatives (**3a-w**) is illustrated in Scheme **2**. The physicochemical properties and their spectroscopic data were reported in our previous publication [18]. All variations of substituents R^1 & R^2 are shown in Table **2**.

3.2. *In vitro* Cholinesterase Inhibition Studies

Ellman's colorimetric method was employed to determine the cholinesterase inhibition potential of the synthesized compounds (**2a-n** & **3a-w**) against AChE and BChE enzymes. Recent studies suggested that in Alzheimer's patients having severe pathology, fluctuation in cholinesterases (AChE & BChE) level occurred in specific regions of the brain [7, 24]. For AChE as well as BChE enzymes, initially, all compounds were screened at 0.1 mM concentration to assess the % inhibition. Compounds with more than 50% inhibition were further analyzed at multiple concentrations and their IC_{50} values were calculated. Galanthamine was used as a standard inhibitor for both enzymes.

As described earlier, the topology of these compounds can be easily modulated by the use of various readily accessible starting materials generating chromenone derivatives with different substitution sites. These newly developed chromenones might be advantageous in the development of cholinesterase inhibitors compared to the literature examples that largely lacked structural diversity and included bulky molecules to inhibit cholinesterase. Screening of chromenone derivatives (**2a-n** & **3a-w**) against AChE and BChE showed that these derivatives exhibited potent inhibitory

Table 1. Cholinesterase inhibition efficacy of compounds 2(a-n).

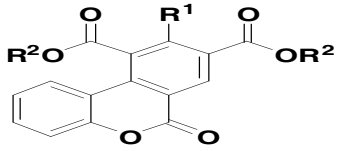

2(a-n)

Sr. No.	R^1	R^2	AChE	BChE
			IC_{50} ± SEM (μM)	
2a	Me	Me	2.03 ± 0.06	2.94 ± 0.08
2b	Et	Me	0.29 ± 0.01	3.82 ± 0.09
2c	OH	Me	0.26 ± 0.01	0.16 ± 0.01
2d	OH	Et	1.78 ± 0.03	0.49 ± 0.01
2e	CH_2Cl	Me	0.98 ± 0.02	0.24 ± 0.01
2f	Me	Et	0.92 ± 0.01	0.51 ± 0.02
2g	Me	*i*-Pr	1.51 ± 0.03	0.43 ± 0.02
2h	Me	$(CH_2)_2OMe$	1.45 ± 0.02	1.39 ± 0.03
2i	Me	Allyl	0.76 ± 0.01	3.63 ± 0.01
2j	Pr	Et	0.25 ± 0.01	0.13 ± 0.02
2k	Me	CH_2Ph	0.53 ± 0.01	3.92 ± 0.02
2l	Ph	Et	0.08 ± 0.03	3.11 ± 0.03
2m	CH_2Cl	Et	0.26 ± 0.01	0.22 ± 0.02
2n	CH_2OMe	Me	1.54 ± 0.03	0.93 ± 0.03
Galanthamine	-	-	0.62 ± 0.01	0.87 ± 0.03

activity (Tables **1** & **2**). Among them, compounds **2l, 3h, 3l, 3o, 3q, 3u** and **3w** were potent inhibitors of AChE, as revealed by experimental data. Diethyl 6-oxo-9-phenyl-6*H*-benzo[*c*]chromene-8,10-dicarboxylate (**2l**) having an IC_{50} value of 0.08 ± 0.03 μM was found to be the most active AChE inhibitor, whereas, **3h, 3l, 3o, 3q, 3u** and **3w** showed significant and comparable IC_{50} values of 0.15 ± 0.01, 0.15 ± 0.01, 0.12 ± 0.01, 0.13 ± 0.01, 0.11 ± 0.01 and 0.11 ± 0.01 μM, respectively. All these inhibitors were more active than the standard galanthamine (0.62 ± 0.01 μM). Substitution patterns of these compounds represented a balance of electronic and steric effects. Similarly, compounds **2c, 2j, 2m, 3h, 3p, 3q, 3r** and **3w** displayed potent BChE inhibitory activity. Among these, **3q** (*tert*-butyl 9-(4-(*tert*-butyl)phenyl)-6-oxo-6*H*-benzo[*c*]chromene-8-carboxylate) having an IC_{50} value of 0.04 ± 0.01 μM was found to be the most potent BChE inhibitor, while the remaining compounds **2c, 2j, 2m, 3h, 3p, 3r** and **3w** exhibited IC_{50} values of 0.16 ± 0.01, 0.13 ± 0.02, 0.22 ± 0.02, 0.09 ± 0.01, 0.15 ± 0.02, 0.07 ± 0.01 and 0.33 ± 0.02 μM, respectively.

Most of the compounds in this series were found to exhibit dual inhibitory activity against AChE and BChE, among which **3h** (ethyl 6-oxo-9-propyl-6*H*-benzo[*c*]chromene-8-carboxylate) and **3q** (*tert*-butyl 9-(4-(*tert*-butyl) phenyl)-6-oxo-6*H*-benzo[*c*]chromene-8-carboxylate) were most potent. The IC_{50} values of **3h** and **3q** were 0.15 ± 0.01 and 0.13 ± 0.01 μM, respectively for AChE and 0.09 ± 0.01 and 0.04 ± 0.01 μM, respectively for BChE (Tables **1** & **2**). In general, all the derivatives showed strong inhibitory potential for AChE and most of them were also potent inhibitors of BChE. Several AChE inhibitors showed improved inhibitory activity compared to standard inhibitor galanthamine and some of the BChE inhibitors displayed the same trend.

The cholinesterase inhibitory profile of the tested compounds was dependent on several factors including the nature of the substituents and their presence at different positions of the basic skeleton. Among the series **2a-n**, compound **2l** was the most potent inhibitor with a phenyl ring at R^1 position while carrying an ethyl group at R^2 position. The presence of a phenyl group increased the inhibition of **2l** to ~8 fold compared to galanthamine. A similar trend was observed for compounds **3a-w**, when a phenyl ring was substituted at R^1, irrespective of the substituent attachment at R^2, an enhanced inhibitory activity was observed (**3d, 3e, 3k**). At the same time, all compounds of both series carrying a

Table 2. Cholinesterase inhibition efficacy of compounds 3(a-w).

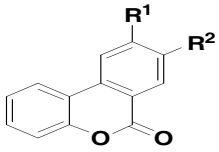

3(a-w)

Sr. No.	R^1	R^2	AChE	BChE
			IC_{50} ± SEM (μM)	
3a	4-MeC_6H_4	CO_2Me	0.76 ± 0.01	0.71 ± 0.02
3b	Ph	CO_2Me	1.67 ± 0.03	2.83 ± 0.09
3c	*n*-Pent	CO_2Me	0.45 ± 0.01	3.41 ± 0.02
3d	Ph	CO_2Et	0.36 ± 0.01	4.37 ± 0.03
3e	Ph	CO_2-*i*-Pr	0.29 ± 0.02	2.79 ± 0.02
3f	*n*-Pent	CO_2Et	0.50 ± 0.01	3.61 ± 0.01
3g	*n*-Pr	CO_2Me	0.42 ± 0.01	2.98 ± 0.03
3h	*n*-Pr	CO_2Et	0.15 ± 0.01	0.09 ± 0.01
3i	*n*-Pr	CO_2-*i*-Pr	0.65 ± 0.01	0.77 ± 0.01
3j	*n*-Pr	COMe	0.40 ± 0.01	0.74 ± 0.02
3k	Ph	COMe	0.25 ± 0.01	1.49 ± 0.01
3l	*n*-Pent	COMe	0.15 ± 0.01	3.53 ± 0.04
3m	4-MeC_6H_4	CO_2Et	0.42 ± 0.01	4.87 ± 0.04
3n	4-MeC_6H_4	COMe	0.41 ± 0.01	3.45 ± 0.02
3o	*t*-BuC_6H_4	CO_2Me	0.12 ± 0.01	2.73 ± 0.03
3p	*t*-BuC_6H_4	CO_2Et	0.22 ± 0.01	0.15 ± 0.02
3q	*t*-BuC_6H_4	CO_2-*t*-Bu	0.13 ± 0.01	0.04 ± 0.01
3r	2-MeC_6H_4	CO_2Me	0.21 ± 0.01	0.07 ± 0.01
3s	4-*n*-PrC_6H_4	CO_2Me	0.43 ± 0.01	7.19 ± 0.05
3t	4-FC_6H_4	CO_2Me	1.85 ± 0.02	5.67 ± 0.04
3u	4-FC_6H_4	CO_2Et	0.11 ± 0.01	4.46 ± 0.03
3v	4-(MeO)C_6H_4	CO_2Me	0.21 ± 0.01	3.24 ± 0.09
3w	4-(MeO)C_6H_4	CO_2Et	0.11 ± 0.01	0.33 ± 0.02
Galanthamine	-	-	0.62 ± 0.01	0.87 ± 0.03

phenyl moiety at R^1 showed significant inhibition of AChE but lower activity against BChE. Moreover, in the series **2a-n**, an ethyl substituent had a greater influence on inhibition against both ChEs and the inhibitory activity of the compounds was found to be higher than that of the standard inhibitor galanthamine. Overall, the compounds in series **2a-n** were found to be more potent against BChE, whereas, compounds of series **3a-w** exhibited significant inhibition of AChE. Although both series shared the same basic skeleton, they contained different substituents, which was a likely reason for variation in the inhibitory activities of both sets of compounds. In the case of **3a-w**, the larger substituents were attached at both positions (R^1 & R^2) while smaller substituents were present in **2a-n**. Substitution patterns are reported in Tables **1** and **2**.

3.4. Molecular Docking

For docking analysis, X-ray structures of human AChE (PDB ID: 4BDT) and BChE (PDB ID: 4BDS) were selected as templates because structures of electric eel AChE were only available at very low crystallographic resolutions (> 4

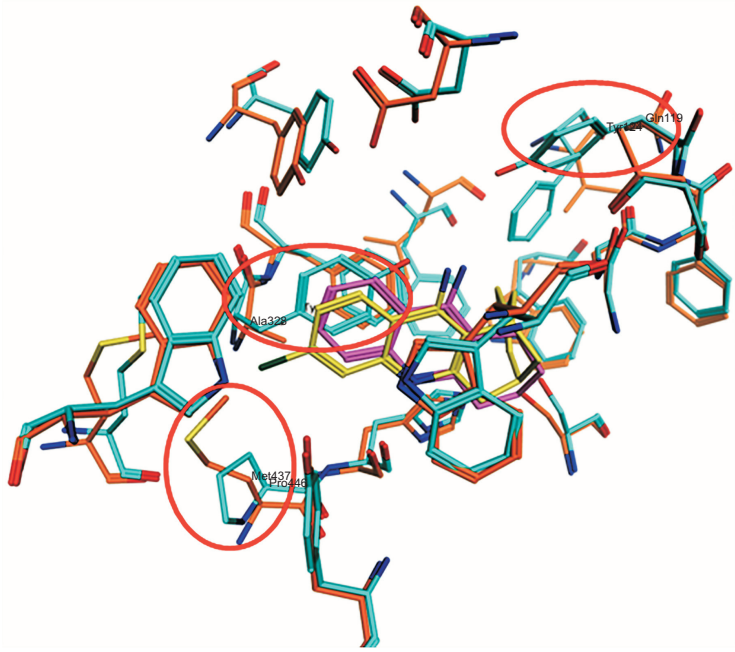

Fig. (1). Comparison of active sites. A superposition of active site residues of X-ray structures of AChE (cyan) in complex with huprine W (yellow) and BChE (orange) in complex with tacrine (magenta) is shown. Circled in red are residue differences in the active sites, as discussed in the text. (For interpretation of the references to color in this figure legend, the reader is referred to the web version of this paper).

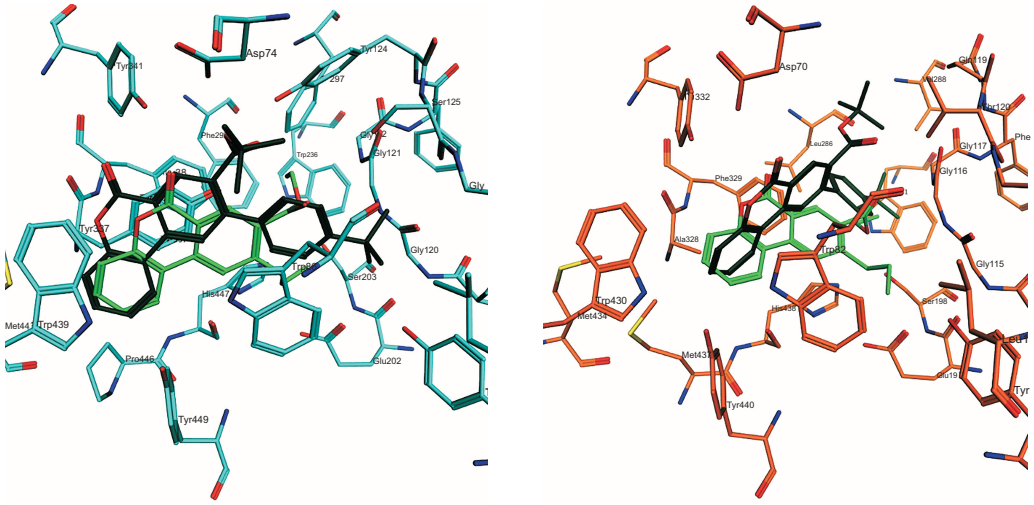

Fig. (2). Putative binding modes. Docking poses of compounds **3h** (light green) and **3q** (dark green) in the active sites of AChE (left) and BChE (right). (For interpretation of the references to color in this figure legend, the reader is referred to the web version of this paper).

Å) and a structure of equine BChE was not available. A comparison of the active sites of AChE and BChE including bound ligands is shown in Fig. (**1**). The residue Tyr337 in AChE is replaced by Ala328 in BChE. For docking, the side chain of Tyr337 in AChE was treated flexibly (as the only residue in both structures) because different X-ray structures revealed multiple side chain conformations of Tyr337 depending on co-crystallized compounds. The corresponding BChE residue Ala328 has no side chain flexibility.

Another notable difference between the active sites is the replacement of residue Pro446 in AChE at the bottom of the hydrophobic pocket by the bulkier residue Met437 in BChE. Furthermore, Tyr124 in AChE is replaced by Gln119 in BChE, which adopts different side chain orientations. The crystallographic ligands huprine W (AChE) and tacrine (BChE) show similar binding modes within the active sites of these enzymes. Huprine W is sandwiched between the aromatic side chains of residues Tyr337 and Trp86 and formed π-π interactions. Due to the replacement of Tyr337 by Ala328 in BChE, formation of the aromatic sandwich is not possible. Nevertheless, the aromatic ring system of tacrine is oriented similarly to the corresponding moiety in huprine W [20].

The best dual AChE/BChE inhibitors identified herein, compounds **3h** and **3q**, were docked into the active sites of the two enzymes. Fig. (**2**) shows an overlay of the putative binding modes of compounds **3h** and **3q** in AChE and BChE. The docking poses are similar, yielding favorable positions of the 6H-benzo[c]chromen-6-one ring systems for interactions with side chains of several aromatic residues.

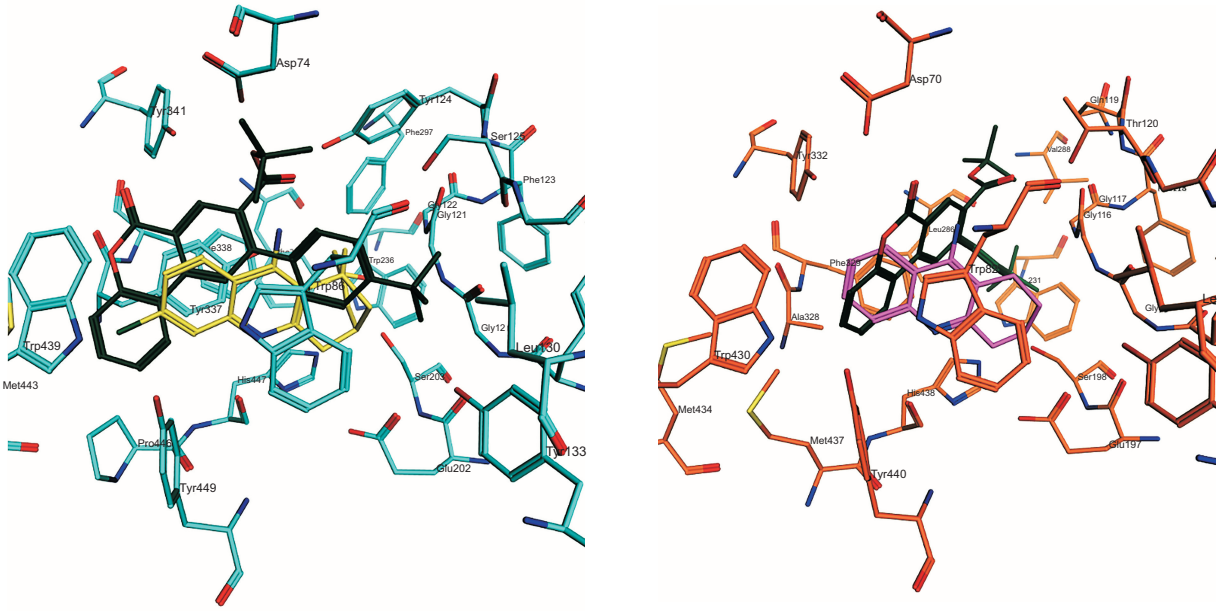

Fig. (3). Putative versus crystallographic binding modes. Overlays of docking poses of compound **3q** (dark green) and the X-ray structure of huprine W (yellow) within the active site of AChE (left) and the X-ray structure of tacrine (magenta) within the active site of BChE (right) are shown. (For interpretation of the references to color in this figure legend, the reader is referred to the web version of this paper).

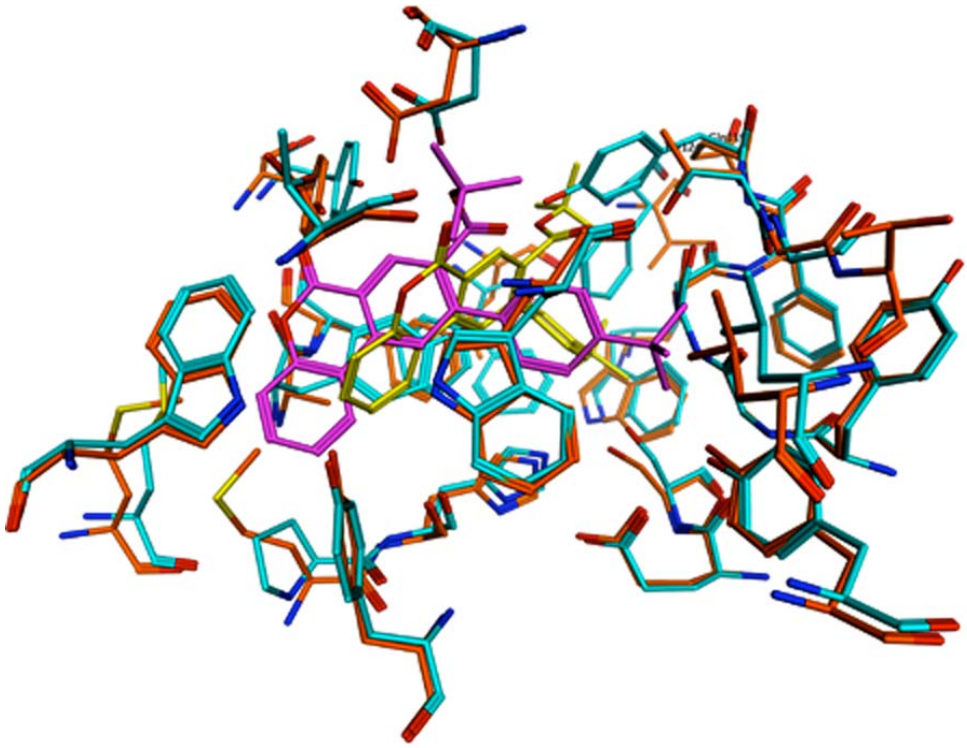

Fig. (4). Comparison of predicted binding modes. Shown is a superposition of active site residues of AChE (cyan) and of BChE (orange) with the respective docking poses of compound **3q** (magenta: **3q** docked into AChE, yellow: **3q** docked into BChE). (For interpretation of the references to color in this figure legend, the reader is referred to the web version of this paper).

In addition, the ring carbonyl groups of both compounds are in potential hydrogen bonding distance to the side chain hydroxyl group of Tyr341 (AChE). In BChE, the ring systems of **3h** and **3q** adopt slightly different positions than in AChE due to the replacement of Tyr337 (AChE) with Ala328 (BChE). The smaller alanine residue leads to a minor ring re-orientation bringing **3h** in possible hydrogen bonding distance to residues Ser198 and His438 of the catalytic triad of BChE. Furthermore, the ethoxy substituent is directed towards a lipophilic pocket formed by residues Val288, Leu286, Phe329 and Trp231. Comparisons of the predicted binding modes of **3q** and the crystallographic huprine W within the active site of AChE and in the active site of hBChE are shown in Fig. (**3**).

In AChE, both **3q** and huprine W adopt a parallel orientation between Tyr337, Trp86 and Trp439, while the ring systems of tacrine and **3q** are not in a parallel arrangement with the active site of BChE. Fig. (**4**) shows a superposition of the putative binding modes of compound **3q** within the active sites of AChE and BChE. Compound **3q** fits more deeply into the hydrophobic pocket formed by the residues Trp86/Trp82 (AChE/BChE), Tyr337/Ala328, Tryp439/ Trp430, Pro446/Met437, and Tyr449/Tyr440 in case of AChE. The reason for the slightly different position is the exchange of the residue Pro446 in AChE at the bottom of the hydrophobic pocket with the bulkier residue Met437 in BChE. Nevertheless, the 6H-benzo[c]chromen-6-one ring systems can interact with the aromatic residues of both enzymes. As a consequence of this rearrangement, different interactions are likely for the inhibitor in the active sites of AChE and BChE, *i.e.,* alternative hydrogen bonds with Tyr341 (AChE) and Thr120 (BChE) might be formed. In addition, the tertiary butyl phenyl substituent of the inhibitor is placed into a hydrophobic pocket formed by residues Val288, Trp231, and Leu286 in the active site of BChE.

This orientation would not be possible within the active site of AChE because of short contacts between the inhibitor and Tyr337, which restricts the available space in AChE compared to BChE and might thus be responsible for partly different compound binding modes.

For both enzymes, plausible binding modes were obtained for compounds **3h** and **3q**, which would be consistent with the comparable potency of these compounds against both enzymes. The aromatic ring systems of the chromene derivatives were in the corresponding position to the crystallographic ligands huprine W (AChE) and tacrine (BChE), which further supports the putative binding modes. Taken together, the results presented herein show that the novel oxo chromene carboxylates are promising inhibitors of cholinesterases, especially BChE, which might be used as an important starting point for further therapeutic investigations of Alzheimer's and related neurodegenerative diseases.

CONCLUSION

Alzheimer's Disease (AD) is complex and multi-factorial in nature. In the past few years, researchers have paid much attention to cholinergic transmission and pathophysiology of AD as a neurodegenerative disease. Hence, in the search for more effective therapeutic agents for AD, we identified new chromenone derivatives (**2a-n** & **3a-w**) and analyzed their acetylcholinesterase and butyrylcholinesterase inhibitory activities. These compounds exhibited significant inhibition of cholinesterases and some of them revealed dual inhibition of AChE and BChE. The possible interactions of the most potent compounds with their enzyme targets were studied by molecular docking of the dual AChE/BChE inhibitors **3h** and **3q**. These potent dual AChE/BChE inhibitors showed favorable orientations within the active sites of the target enzymes. Therefore, these inhibitors of AChE/BChE may be considered for the treatment of neurodegenerative disorders including Alzheimer's and age-related cholinesterase damage.

ETHICS APPROVAL AND CONSENT TO PARTICIPATE

Not applicable.

HUMAN AND ANIMAL RIGHTS

No Animals/Humans were used for studies that are base of this research.

CONSENT FOR PUBLICATION

Not applicable.

CONFLICT OF INTEREST

The authors declare no conflict of interest, financial or otherwise.

ACKNOWLEDGEMENTS

Jamshed Iqbal is thankful to the Organization for the Prohibition of Chemical Weapons (OPCW), The Hague, The Netherlands and Higher Education Commission of Pakistan for the financial support through Project No. 20-3733/ NRPU/R&D/14/520. N.F. was supported by a fellowship from the Jürgen Manchot Foundation, Düsseldorf, Germany.

REFERENCES

[1] Saeed, A.; Mahesar, P.A.; Zaib, S.; Khan, M.S.; Matin, A.; Shahid, M.; Iqbal, J. Synthesis, cytotoxicity and molecular modelling studies of new phenylcinnamide derivatives as potent inhibitors of cholinesterases. *Eur. J. Med. Chem.,* **2014**, *78*, 43-53.

[2] Budson, A.E.; Solomon, P.R. New diagnostic criteria for Alzheimer's disease and mild cognitive impairment for the practical neurologist. *Pract. Neurol.,* **2012**, *12,* 88-96.

[3] Alptüzün, V.; Prinz, M.; Hörr, V.; Scheiber, J.; Radacki, K.; Fallarero, A.; Vuorela, P.; Engels, B.; Braunschweig, H.; Erciyas, E. Interaction of (benzylidene-hydrazono)-1, 4-dihydropyridines with β-amyloid, acetylcholine, and butyrylcholine esterases. *Bioorg. Med. Chem.,* **2010**, *18,* 2049-2059.

[4] Quinn, D.M. Acetylcholinesterase: Enzyme structure, reaction dynamics, and virtual transition states. *Chem., Rev.,* **1987**, *87,* 955-979.

[5] Shah, M.S.; Khan, S.U.; Ejaz, S.A.; Afridi, S.; Rizvi, S.U.F.; Najam-ul-Haq, M.; Iqbal, J. Cholinesterases inhibition and molecular modeling studies of piperidyl-thienyl and 2-pyrazoline derivatives of chalcones. *Biochem. Biophys. Res. Commun.,* **2017**, *482,* 615-624.

[6] Zhang, X. Cholinergic activity and amyloid precursor protein processing in aging and Alzheimer's disease. *Curr. Drug Targets-CNS Neurol. Disord*., **2004**, *3,* 137-152.

[7] Giacobini, E. Butyrylcholinesterase: Its function and inhibitors. *Taylor & Francis,* **2003**.

[8] Bierer, L.M.; Haroutunian, V.; Gabriel, S.; Knott, P.J.; Carlin, L.S.; Purohit, D.P.; Perl, D.P.; Schmeidler, J.; Kanof, P.; Davis, K.C. Neurochemical correlates of dementia severity in Alzheimer's disease: relative importance of the cholinergic deficits. *J. Neurochem.,* **1995**, *64,* 749-760.

[9] Wu, C.K.; Thal, L.; Pizzo, D.; Hansen, L.; Masliah, E.; Geula, C. Apoptotic signals within the basal forebrain cholinergic neurons in Alzheimer's disease. *Exp. Neurol.,* **2005**, *195*, 484-496.

[10] Gron, G.; Brandenburg, I.; Wunderlich, A.P.; Riepe, M.W. Inhibition of hippocampal function in mild cognitive impairment: targeting the cholinergic hypothesis. *Neurobiol. Aging,* **2006**, *27,* 78-87.

[11] Ul-Haq, Z.; Khan, W.; Kalsoom, S.; Ansari, F.L. *In silico* modeling of the specific inhibitory potential of thiophene-2, 3-dihydro-1, 5-benzothiazepine against BChE in the formation of β-amyloid plaques. *Theoret. Biol. Med. Modell.,* **2010**, *7,* 22.

[12] Greig, N.H.; Utsuki, T.; Yu, Q.-S.; Zhu, X.; Holloway, H.W.; Perry, T.; Lee, B.; Ingram, D.K.; Lahiri, D.K. A new therapeutic

target in Alzheimer's disease treatment: attention to butyrylcholinesterase. *Curr. Med. Res. Opin.,* **2001**, *17,* 159-165.

[13] Zawadzka, A.; Łozińska, I.; Molęda, Z.; Panasiewicz, M.; Czarnocki, Z. Highly selective inhibition of butyrylcholinesterase by a novel melatonin–tacrine heterodimers. *J. Pineal Res.,* **2013**, *54,* 435-441.

[14] Schneider, L.S. Treatment of Alzheimer's disease with cholinesterase inhibitors. *Clin. Geriatric Med.,* **2001**, *17,* 337-358.

[15] Najafi, Z.; Saeedi, M.; Mahdavi, M.; Sabourian, R.; Khanavi, M.; Tehrani, M.B.; Moghadam, F.H.; Edraki, N.; Karimpor- Razkenari, E.; Sharifzadeh, M.; Foroumadi, A.; Shafiee, A.; Akbarzadeh, T. Design and synthesis of novel anti-Alzheimer's agents: Acridine-chromenone and quinoline-chromenone hybrids. *Bioorg. Chem.,* **2016**, *67,* 84-94.

[16] Saeedi, M.; Safavi, M.; Karimpour-Razkenari, E.; Mahdavi, M.; Edraki, N.; Moghadam, H.; Khanavi, M.; Akbarzadeh, T. Synthesis of novel chromenones linked to 1, 2, 3-triazole ring system: Investigation of biological activities against Alzheimer's disease. *Bioorg. Chem.,* **2017**, *70,* 86-93.

[17] Iaroshenko, V.O.; Abbasi, M.S.A.; Villinger, A.; Langer. P. Synthesis of 6H-benzo [c] chromen-6-ones by cyclocondensation of 1, 3-dicarbonyl compounds with 4-chloro-3-formylcoumarin. *Tetrahedron Lett.,* **2011**, *52,* 5910-5912.

[18] Iaroshenko, V.O.; Abbasi, M.S.A.; Villinger, A.; Langer, P. One-pot synthesis of biaryl lactones by sonogashira cross-coupling reactions of 4-chloro-3-formylcoumarin and subsequent domino [5+1] cyclization/deacetylation reactions with 1,3-dicarbonyl compounds. *Adv. Syn. Catal.,* **2012**, *354,* 803-806.

[19] Ellman, G.L.; Courtney, K.D.; Andres, V.; Featherstone, R.M. A new and rapid colorimetric determination of acetylcholinesterase activity. *Biochem. Pharmacol.,* **1961**, *7,* 88IN191-9095.

[20] Nachon, F.; Carletti, E.; Ronco, C.; Trovaslet, M.; Nicolet, Y.; Jean, L.; Renard, P.-Y. Crystal structures of human cholinesterases in complex with huprine W and tacrine: Elements of specificity for anti-Alzheimer's drugs targeting acetyl-and butyryl-cholinesterase. *Biochem. J.,* **2013**, *453,* 393-399.

[21] RCSB Protein Data Bank. Available at: http://www.rcsb.org (accessed March 1, **2013**)

[22] Morris, G.M.; Huey, R.; Lindstrom, W.; Sanner, M.F.; Belew, R.K.; Goodsell, D.S.; Olson, A.J. AutoDock4 and AutoDockTools4: Automated docking with selective receptor flexibility. *J. Comput. Chem.,* **2009**, *30*, 2785-2791.

[23] Molecular Operating Environment (MOE), 2012.10; Chemical Computing Group Inc., Montreal, Canada.

[24] Kuhl, D.E.; Koeppe, R.A.; Snyder, S.E.; Minoshima, S.; Frey, K.A.; Kilbourn, M.R. *In vivo* butyrylcholinesterase activity is not increased in Alzheimer's disease synapses. *Ann. Neurol.,* **2006**, *59,* 13-20.